Synergism of Calcium and Carbohydrate Binding to Mammalian Lectin

William E. Harte, Jr.,* and Jurgen Bajorath†

Contribution from the Bristol-Myers Squibb Pharmaceutical Research Institute, 5 Research Parkway, Wallingford, Connecticut 06492

Received December 21, 1993. Revised Manuscript Received July 26, 1994⊗

Abstract: The C-type lectin domain of the rat mannose-binding protein contains a complex network of protein−carbohydrate−calcium−water interactions. The crystallographic geometry of the binding site was reproduced by molecular dynamics simulation. The integrity of the binding site geometry, however, is critically dependent on the presence of a third calcium ion in the mannose-binding protein. This ion is distant from the bound carbohydrate, and its presence was originally considered to be a crystallization artifact. A network of concerted motions spanning spatially distant secondary structure elements in the lectin domain was observed in the dynamical model only when the third calcium binding site was occupied. This cooperativity may be implicated in ligand binding stabilization.

Introduction

The carbohydrate-recognition domain (CRD) of the rat mannose-binding protein (MBP) is the first member of the family of C-type (or calcium-dependent) mammalian lectins[1] for which a three-dimensional structure has been reported.[2] CRD or CRD-like domains are part of many mammalian mannose-binding proteins and other carbohydrate-binding proteins with distinct specificity[1] such as the selectins, a family of cellular adhesion molecules.[3] Carbohydrate binding to this family of proteins is strictly calcium dependent. For the rat mannose-binding protein, binding studies suggested that two calcium or holmium cations are required to stabilize the binding of its high-mannose ligand.[4] Consistent with these results, the crystal structure of the MBP apoprotein, determined as a complex where calcium was replaced by holmium, displayed two holmium binding sites (sites 1 and 2).[2] A subsequent crystallographic analysis of MBP complex with a high-mannose ligand,[5] now in calcium- rather than holmium-bound form, revealed an additional calcium binding site (3), 11.6 Å distant from calcium binding site 2.[5] Calcium 2 (Cs2) was found to directly bind the terminal mannose unit of the oligosaccharide ligand in a previously unobserved fashion.[5] Calcium ions 1 (Ca1) and 3 (Ca3) bind to MBP in close proximity (3.9 Å) and share two amino acid ligands. In addition, four water molecules were found to participate in the heptacoordination of Ca3. From these observations, together with the previously reported binding data,[4] Weis et al. concluded that the binding of Ca3 was due to the presence of excess calcium under crystallization conditions.[5] Ca3 was, therefore, considered to be a "nonfunctional" calcium binding site.

We sought to develop a dynamical model of the MBP complex which involves complex interactions of protein and carbohydrate atoms, calcium ions, and water molecules and report here the results of molecular dynamics (MD) simulations on a solvated form of the crystallographic complex. We have simulated, under identical protocols, the MBP−mannose complex in the presence (Ca1−2−3 complex) as well as in the absence (Ca1−2 complex) of the nonfunctional Ca3. We find better agreement with the observed crystallographic data in the simulation of the Ca1−2−3 complex (i.e., in the presence of the third nonfunctional calcium) than in the simulation of the Ca1−2 complex. The analysis of the MD trajectory of the Ca1−2−3 complex reveals a network of correlated motions within the complex which is not found in the simulated Ca1−2 complex. Finally, we sought to propose an experimentally testable hypothesis. We simulated the Asp194-Asn194 (D194N) mutant of MBP in the presence of all three calciums in order to observe the effect of weakening the protein coordination sphere of Ca3. The results were essentially identical to those for the Ca1−2 complex, including poorer agreement with the observed crystallographic data and a lack of correlated motion. The results suggest an unexpected direct functional role of Ca3 in carbohydrate binding to MBP via through-sphere interactions. This hypothesis is experimentally testable as the D194N mutant is proposed to affect the function of the mannose-binding protein.

Methods

Molecular Dynamics. The point of departure for each MD was the X-ray crystal structure of MBP complexed with a monosaccharide of mannose, simplified from the oligosaccharide solved and either all three crystallographically observed calcium ions or the complex with calciunm ion 3 removed. In the D194N mutant Asp194 was converted to the isostructural Asn194. Molecular dynamics calculations in this study were performed with the Monte Carlo (MC) and MD simulation program WESDYN 1.0[6] using the GROMOS86[7] force field and the SPC[8] model for water. All ionizable residues were assumed to be in the form prevalent at physiological pH. Switching functions were used to make the long-range nonbonded interactions vanish smoothly between 7.5 and 8.5 Å, and applied on a group by group basis to avoid artificially splitting dipoles. The protein was solvated with either 3876 or 3877 (to replace the missing calcium) molecules of water in a

* Address correspondence to W. Harte, BMS-PRI, 5 Research Pkwy., Wallingford, CT 06492. Fax: (203) 284-7702. Tel: (203) 284-6913.
† Present address: 3005 First Ave., Seattle, WA 98121.
⊗ Abstract published in *Advance ACS Abstracts*, October 1, 1994.

(1) Drickamer, K. *J. Biol. Chem.* **1988**, *263*, 9557−9560.
(2) Weis, W. I.; Kahn, R.; Fourme, R.; Drickamer, K.; Hendrickson, W. A. *Science 254*, **1991**, 1608−1615.
(3) Lasky, L. A. *Science* **1992**, *258*, 964−969.
(4) Weis, W. I.; Crichlow, G. V.; Krishna Murthy, H. M.; Hendrickson, W. A.; Drickamer, K. *J. Biol. Chem.* **1991**, *266*, 20678−20686.
(5) Weis, W. I.; Drickamer, K.; Hendrickson, W. A. *Nature* **1992**, *360*, 127−134.
(6) Swaminathan, S. WESDYN, Wesleyan University, 1990.
(7) van Gunsteren, W. F.; Berendsen, H. J. C. GROMOS86, University of Groningen, 1986.
(8) Berendsen, H. J. C.; Postma, J. P. M.; van Gunsteren, W. F.; Hermans, J. In *Intermolecular Forces*; Pullman, B., Ed.; D. Reidel: Dordrecht, The Netherlands, 1981.

0002-7863/94/1516-10394$04.50/0

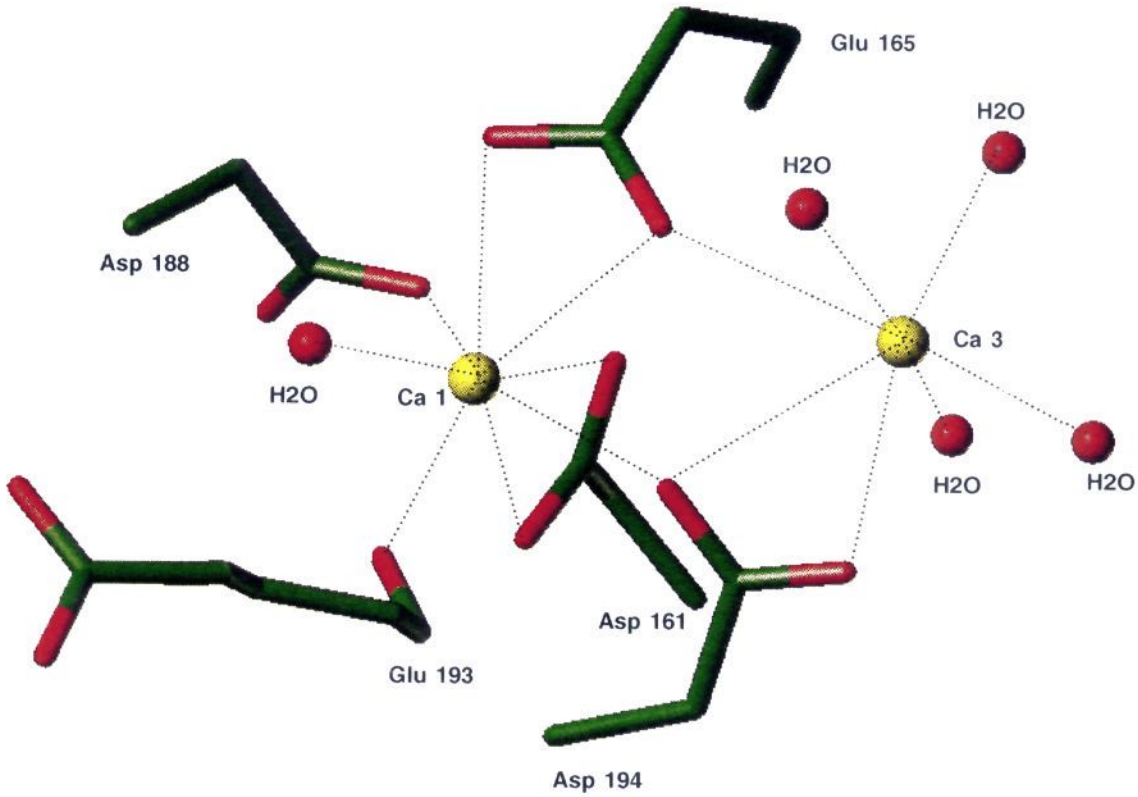

Figure 1. Simulated calcium coordination spheres in MBP. The coordination of calcium ions 1 and 3 in the dynamical MBP model is shown. Dashed lines denote calcium coordination bonds. In the experimental structure, both calciums are heptacoordinated in a distorted pentagonal bipyramid. This coordination sphere is found to be essentially conserved in the simulation. In the dynamical model, water molecules were considered as a ligand only if their isotropic temperature factor (calculated from the MD trajectory) was less than 30 Å^2.

hexagonal prism cell with a height of 56.543 Å and radius of the hexagon of 30.565 Å, and treated under periodic boundary conditions in the MD. The volume of the system was chosen to produce a solvent density of 1 g/cm^3. The simulations in each case involved an initial solvent relaxation of 3000 passes of Metropolis MC (~12 million configurations), followed by 50 steps of conjugate gradient minimization on the total system. The MD involved heating to 300 K over 1.5 ps, a Gaussian equilibration step of 2.5 ps, and 96 ps of free MD under a temperature window of 5 K. No rescaling was required beyond 25 ps into any of the runs, indicative of intrinsic stability in the calculated dynamical structure. Analysis of results was based on the interval between 25 and 100 ps of the trajectory, and included the determination of the average structure over the last 50 ps of the trajectory along with the isotropic temperature factors for each atom. Comparison of the MD results with the corresponding crystal structure data was accomplished by a root mean square (RMS) superposition of the protein backbone residues (109−221). The relatively small backbone RMS deviations of approximately 1.2 Å for all three complexes, relative to the crystallographic data, after 100 ps of MD simulation indicate that the dynamical structure of MBP remained in the realm of the crystal geometry during the course of the simulation, and is further evidence of the inherent stability of the model.

Results and Discussion

For all three simulations the total energy and temperature were observed to be stable after equilibration of approximately of approximately 25 ps. After 100 ps of MD simulation, the protein in both Ca1−2 and Ca1−2−3 complexes as well as the D194N mutant showed overall good agreement with the crystallographic data, yielding comparable backbone RSM deviations of 1.2, 1.1, and 1.1 Å, respectively.

A more detailed comparison of the experimental and simulated calcium binding sites 1 and 3 of the Ca1−2−3 complex (Figure 1) shows the close agreement of Ca coordination spheres in the dynamic and crystallographic models including the coordinated water molecules. Table 1 lists the coordinating atom distances and temperature factors for both the X-ray- and MD-derived model structures.

The two dynamical models of the Ca1−2 and Ca1−2−3 complexes showed a significant difference in the average geometries of the mannose−Ca2−MBP coordination spheres relative to the crystal structure (Figure 2). The major change observed is the average geometry of the mannose. The residual RMS deviation of the mannose monomer is 1.4 Å for the Ca1−2−3 complex and 2.7 Å for the Ca1−2 complex. In the Ca1−2 complex, the calcium coordination sphere is not conserved as both Asn205 and O3 of mannose are no longer ligands for the calcium ion (5.7 and 3.7 Å, respectively). The position of the mannose can roughly be viewed as a 90° rotation from its

(9) (a) Harte, W. E., Jr.; Swaminathan, S.; Mansuri, M. M.; Martin, J. C.; Rosenberg, I. E.; Beveridge, D. L. *Proc. Natl. Acad. Sci. U.S.A.* **1990**, *87*, 8864−8868. (b) Swaminathan, S.; Harte, W. E., Jr.; Beveridge, D. L. *J. Am. Chem. Soc.* **1990**, *113*, 2717−2721. Movements are positively correlated (regions moving in the same direction) or negatively correlated (motions are occurring in opposite directions). Correlated motions can occur among proximal residues comprising well-defined domain regions of secondary structure, and also between regions demonstrating domain−domain communication. The extent of correlated motion is indicated by the magnitude of the corresponding correlation coefficient. The cross-correlation coefficient for the displacement of any two atoms i and j is given by $C_{ij} = \langle \Delta r_i \cdot \Delta r_j \rangle / (\langle \Delta r_i^2 \rangle \langle \Delta r_j^2 \rangle)^{1/2}$, where Δr_i and Δr_j are the displacements from the mean position of the ith and jth atoms. The elements C_{ij} can be collected in matrix form and displayed as a three-dimensional dynamical cross-correlation map (DCCM). The C_{ij} are computed as averages over successive backbone N, Cα, and C atoms to give one entry per pair of amino acid residues. There is a time scale implicit in the C_{ij} as well. DCCMs for all three MBP simulations were calculated as block averages from the MD trajectory over intervals of time from 5 to 25 ps. The mean of three 25-ps block averages is represented in the DCCMs shown in Figure 3.

(10) Kraulis, P. J. *J. Appl. Crystallogr.* **1991**, *24*, 946−950.

Table 1. Calcium Coordination Distance and Temperature Factor

	crystal structure, Å (Å²)	MD simulation Ca1−2−3, Å (Å²)		crystal structure, Å (Å²)	MD simulation Ca1−2−3, Å (Å²)
Ca1	**(14.2)**	**(5.2)**	Asn205		
Asp161			OD1	2.41 (15.3)	3.50 (46.3)
OD1	2.69 (10.6)	2.73 (7.0)	Asp206		
OD2	2.47 (14.0)	2.60 (6.3)	OD1	2.38 (16.6)	2.56 (9.4)
Glu165			mannose		
OE1	2.55 (13.3)	2.58 (7.0)	O3	2.45 (27.3)	3.02 (27.4)
OE2	2.55 (15.3)	2.62 (7.5)	O4	2.54 (20.3)	2.33 (27.3)
Asp188			**Ca3**	**(11.5)**	**(10.0)**
OD1	2.54 (14.7)	2.59 (12.1)	Glu165		
Glu193			OE1	2.27 (13.3)	2.90 (7.1)
O	2.38 (10.7)	2.43 (6.7)	Asp194		
H_2O	2.40 (20.8)	2.43 (6.0)	OD1	2.56 (13.8)	2.90 (6.1)
Ca2	**(17.3)**	**(7.1)**	OD2	2.47 (15.0)	2.52 (10.7)
Glu185			H_2O	2.39 (31.2)	2.40 (19.6)
OE1	2.67 (24.0)	2.61 (12.8)	H_2O	2.24 (36.9)	2.31 (14.8)
Asn187			H_2O	2.27 (30.3)	2.36 (12.2)
OD1	2.47 (18.6)	2.39 (9.3)	H_2O	2.37 (27.2)	2.38 (14.7)
Glu193					
OE1	2.31 (16.4)	2.67 (9.3)			

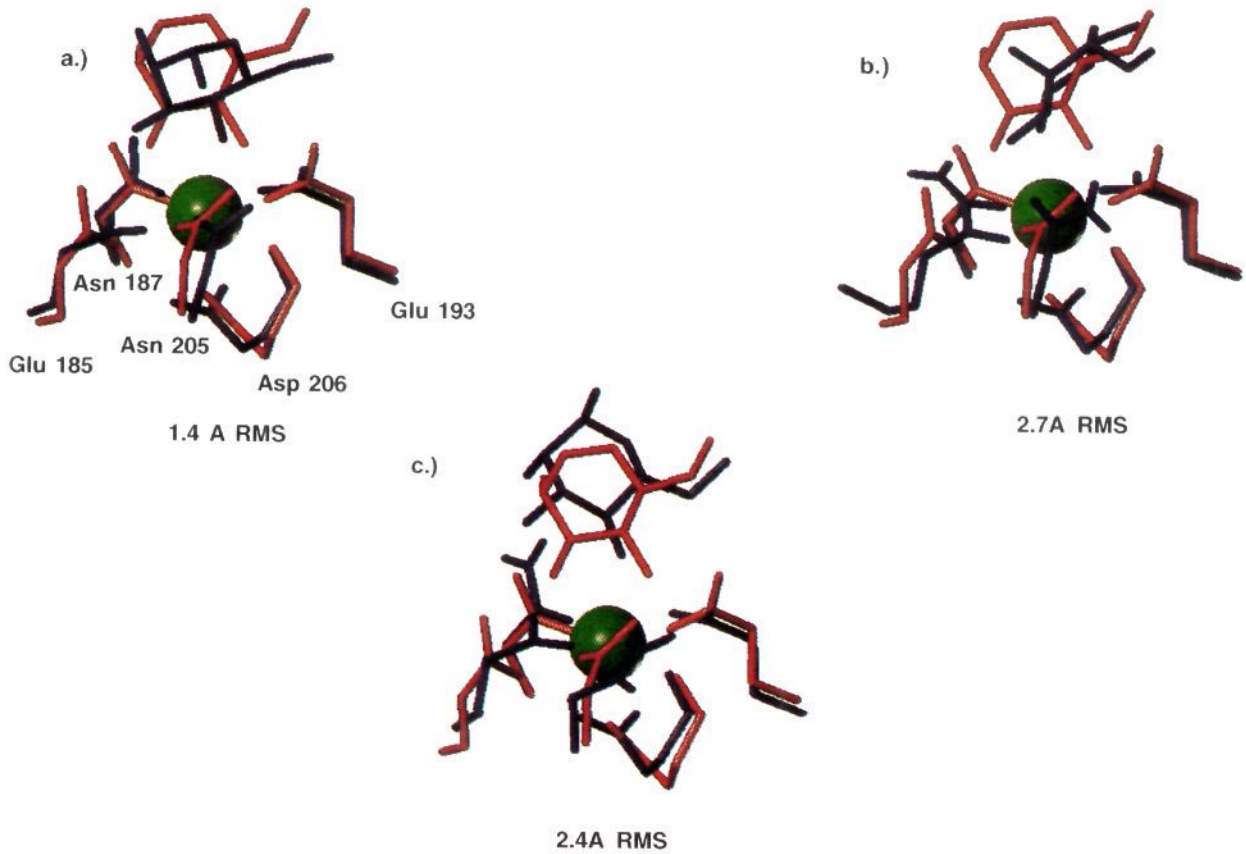

Figure 2. Ca2 coordination sphere in average structures of the MD simulation of (a) Ca1−2−3, (b) Ca1−2, and (c) D194N mutant (green) compared to the X-ray structure (red, ref 7). Superposition of the dynamical and X-ray structures included only the protein backbone atoms. The residual RMS deviation is reported for the heavy atoms of mannose. Structural comparison with the crystallographic model was accomplished by RMS superposition of the protein backbone residues.

crystallographic counterpart. The dynamical model of the Ca1−2 complex, therefore, suggests that the presence of Ca1 and Ca2 may not be sufficient to stabilize mannose binding to MBP. In constrast, the calcium coordination in the simulation of the Ca1−2−3 complex is stable and very similar to the crystallographic coordination. In addition to coordinating calcium, mannose O3 and O4 are involved in hydrogen bonding to Glu193 and Glu185, respectively. The D194N mutant also shows significant deviation from the X-ray geometry, 2.4 Å. Again, Asn205 and O3 of mannose are no longer ligands for the calcium ion. Ca3 moved 4 Å from the observed binding site, removing its electrostatic contribution from the protein system. It follows that Ca3, albeit distant from the Ca2 coordination sphere and mannose binding site, may play an unexpected role in the stabilization of mannose binding to MBP.

Correlated motions within the dynamical protein models were obtained from the MD trajectories using a previously described methodology.[9] This method assesses the correlated motion with

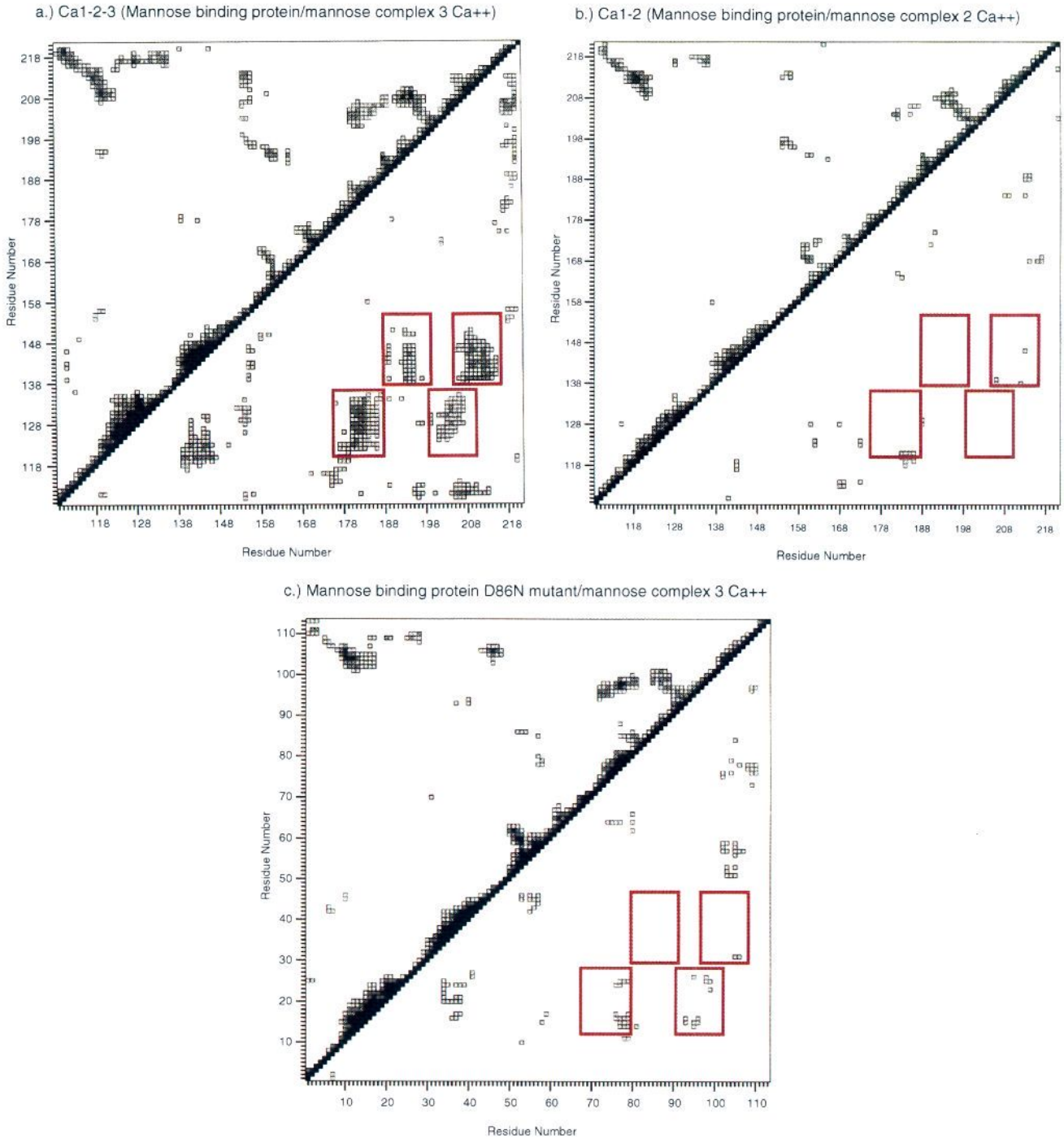

Figure 3. Calculated DCCM for the (a) Ca1−2−3, (b) Ca1−2, and (c) D194N complexes averaged over the 25−100-ps interval of the simulation, block averaged over 25 ps. *Long-distance communication is highlighted in red.* Only correlations >0.25 (3σ) are shown, and the intensity of shading is proportional to the size of the cross-correlation coefficient for each element, as indicated by the key at the top. Positive correlations are shown above the diagonal, and negative correlations are shown below the diagonal. Regions of regular secondary structure are expected to move in concert. Domains of contiguous residues as in an α-helix or β-sheet give rise to regions of significant positive correlations emanating from the diagonal of the DCCM. The two large triangles emanating from the diagonal into the upper half of the DCCM are diagnostic of the α-helices from regions 120−133 and 141−151. The width of a plume represents correlation of proximal residues in the α-helix, and motion appears correlated throughout the entire region. Specific off-diagonal peaks in the DCCM are indicative of regular secondary structure comprised of residues noncontiguous in the amino acid sequence. The major cross-peaks were found in the area of the DCCM between residues 109−119 and 208−220, indicating the C- and N-terminal β-sheets, and between residues 188−198 and 198−208 which fold to form an antiparallel β-sheet containing a small loop region.

the dynamical model and presents the result in a two-dimensional plot, dynamical cross-correlation map (DCCM), somewhat analogous to a 2D NMR experiment. A striking feature of the two DCCM plots in Figure 3 is the lack of correlation in both the Ca1−2 complex and D194N complex compared to the Ca1−2−3 complex (i.e., no significant off-diagonal "islands" of correlation, highlighted in red). The existence of distinct cooperative motions is present only in the Ca1−2−3 complex. Short-range correlated motions were found in all secondary structure elements of the Ca1−2−3 complex.

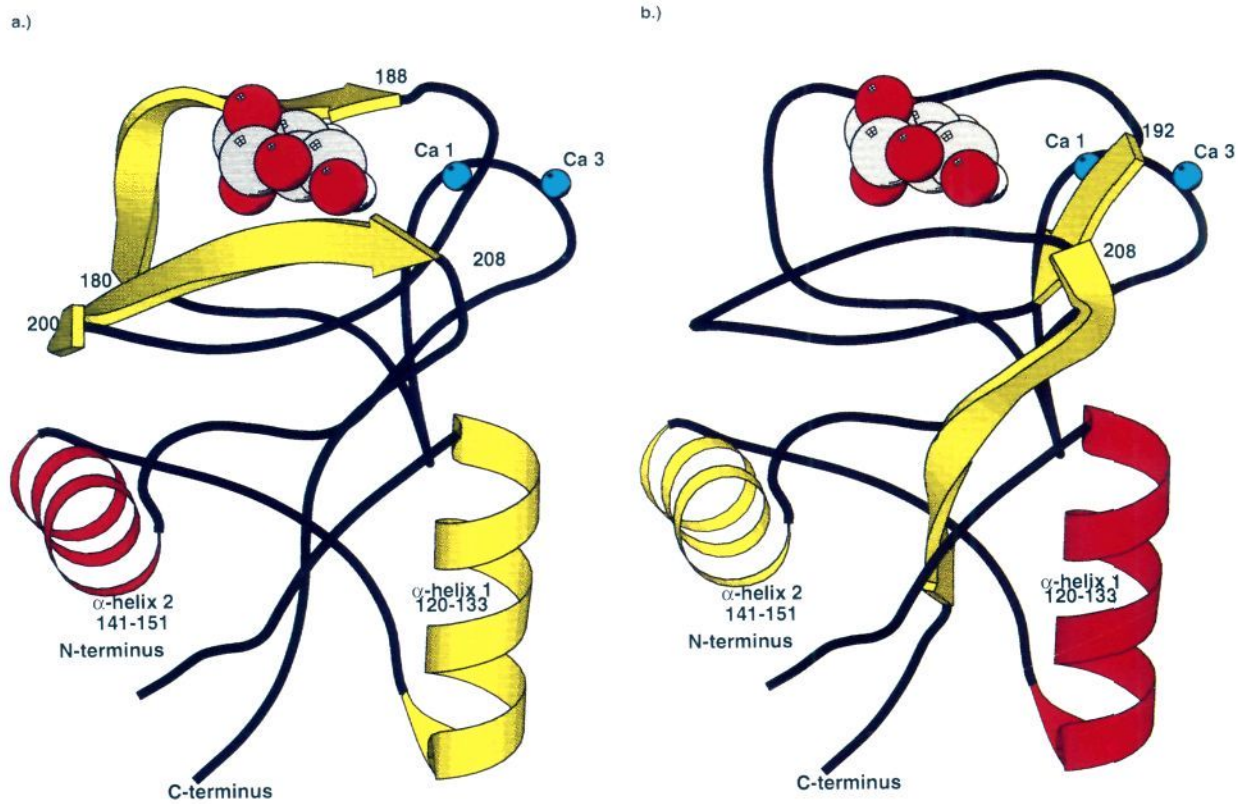

Figure 4. Illustration of long-distance correlated motions in the dynamical model of the Ca1−2−3 complex. (a) Correlations involving α-helix 1. α-Helix 1 (yellow) is correlated to α-helix 2. α-Helix 1 is additionally correlated to regions surrounding the mannose binding site (highlighted in yellow). (b) α-Helix 2 (yellow) is correlated to α-helix 1. α-Helix 2 is additionally correlated to regions surrounding the calcium binding site 1 and a β-sheet near the carboxy terminus (both highlighted in yellow). Many of the interdomain correlations represent communication over a distance >20 Å. Such interdomain correlations are not evident from inspection of the average structure of the protein and can be observed only from MD simulation. Panels a and b were made with the program MOLSCRIPT.[10]

The observed long-range correlations are illustrated in Figure 4. The two helices are strongly correlated, with helix one (120−133) being additionally correlated to residues 180−188 and 200−208. These latter regions comprise the mannose binding site (Figure 4a). Helix 2 (141−151) is additionally correlated to a small region, 192−195 (binding site for calcium 1), and a larger region, 208−217 (Figure 4b). The concerted long-range motions involving the mannose binding site observed in the Ca1−2−3 complex stabilize the MBP−mannose complex according to the dynamical model.

In the dynamical model of the Ca1−2−3 complex, the carbohydrate binding site region is affected by long-distance correlated motions which involve spatially distant secondary structure elements and the water structure around the protein. However, the presence or absence of the third calcium whose coordination involves four water molecules does not lead to significant "short-range" structural perturbations between the calcium binding sites. Indeed, the crystal structures of the apoprotein and mannose complex are virtually superimposible in this region. The distortions of the binding site geometry cannot be explained from a "static" point of view. The dynamical models discussed here provide some insight into the nature of "long-range effects" in proteins which, by means of relatively subtle changes in the dynamic equilibrium of the structure, affect function in the absence of significant conformational changes observable in time-averaged models such as provided by X-ray crystallography.